

topological semimetals in inversion asymmetric systems

Shuichi Murakami

Department of Physics, Tokyo Tech.

TIES, Tokyo Tech.

CREST, JST

Inversion **a**symmetric systems

i.e. chiral systems: Te (tellurium)

- Weyl semimetals
- Chiral transport in crystals with chiral lattice structure

Hirayama, Okugawa, Ishibashi, SM, Miyake, PRL 114, 206401 (2015)

Yoda, Yokoyama, SM, Sci. Rep. 5, 12024 (2015)

Collaborators:

- Tokyo Tech.

M. Hirayama, T. Yoda, T. Yokoyama, R. Okugawa

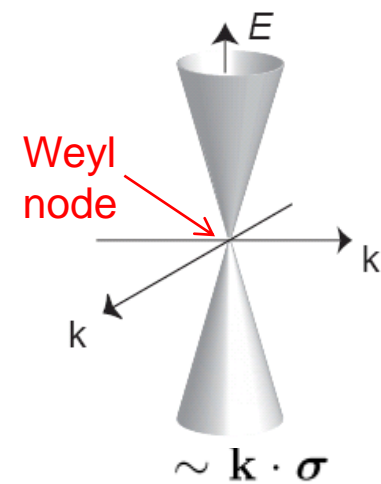
- AIST, Tsukuba, Japan

T. Miyake, S. Ishibashi

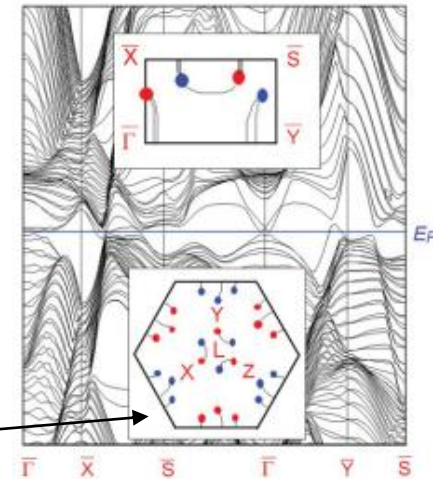
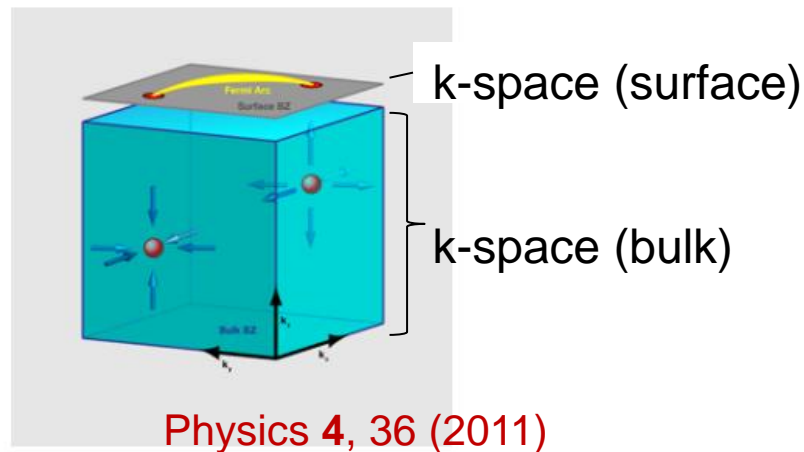
Weyl semimetal

Weyl semimetal = Bulk 3D Dirac cones **without** degeneracy either **time-reversal** or **inversion** symmetry must be broken

(Dirac semimetal = Bulk 3D Dirac cones **with** degeneracy)



- Surface Fermi arc – connecting between Weyl nodes



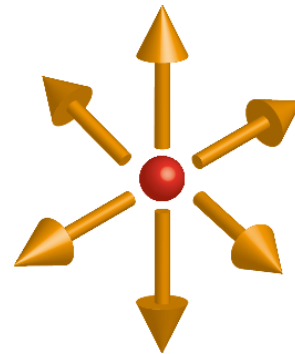
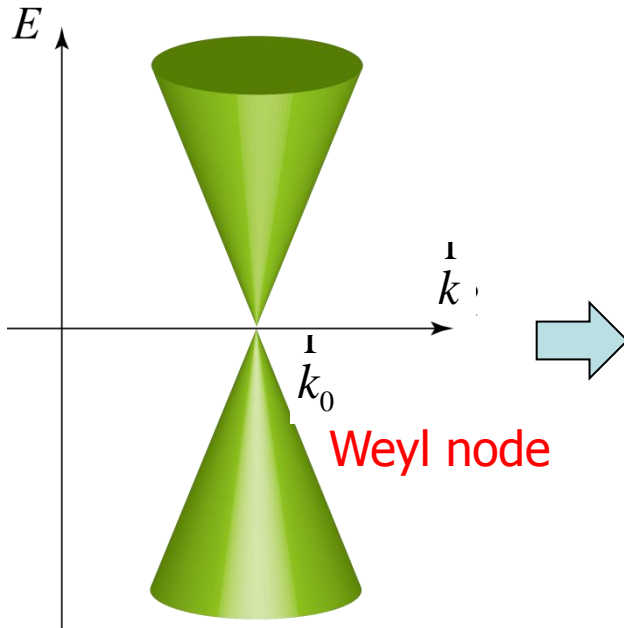
24 Weyl points predicted in $Y_2Ir_2O_7$

- pyrochlore iridates (Wan et al., PRB (2011), Yang et al., PRB(2011))
- TI multilayer (Burkov, Balents)
- TaAs

Wan et al., PRB (2011)

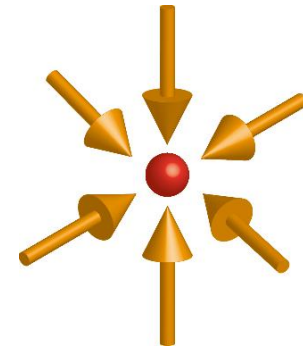
3D Weyl nodes

$$\left\{ \begin{array}{l} B_n(\vec{k}) = i \left\langle \frac{\nabla_{\vec{k}} u_{nk}}{\|\nabla_{\vec{k}} u_{nk}\|}, \frac{\nabla_{\vec{k}} u_{nk}}{\|\nabla_{\vec{k}} u_{nk}\|} \right\rangle : \text{Berry curvature} \\ \rho_n(\vec{k}) = \frac{1}{2\pi} \nabla_{\vec{k}} \cdot \vec{B}_n(\vec{k}) : \text{monopole density} \end{array} \right.$$



Monopole at $\vec{k} = \vec{k}_0$
 $\rho_l(\vec{k}) = \delta(\vec{k} - \vec{k}_0)$

or



Antimonopole at $\vec{k} = \vec{k}_0$
 $\rho_l(\vec{k}) = -\delta(\vec{k} - \vec{k}_0)$

- Weyl nodes are **either monopole or antimonopole**
- Quantized monopole charge

C. Herring, Phys. Rev. 52, 365 (1937).

G. E. Volovik, The Universe in a Helium Droplet (2007).

S. Murakami, New J. Phys. 9, 356 (2007).

Weyl nodes in 2D and 3D

2D Weyl node :

$$H(\mathbf{k}, m) = k_x s_x + k_y s_y$$

parameter m opens a gap.

3D Weyl node :

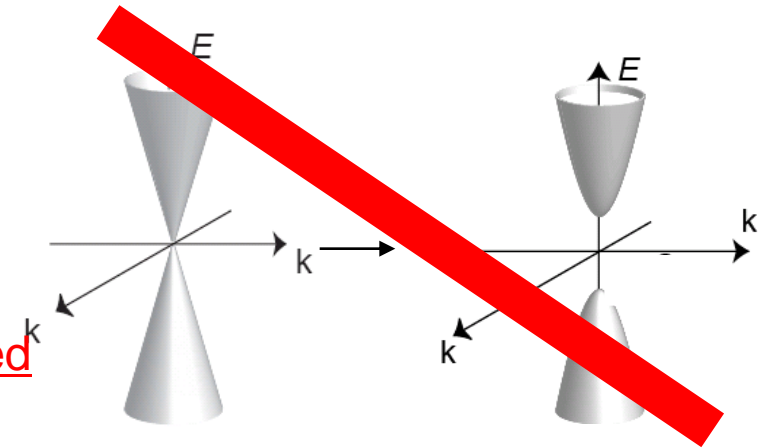
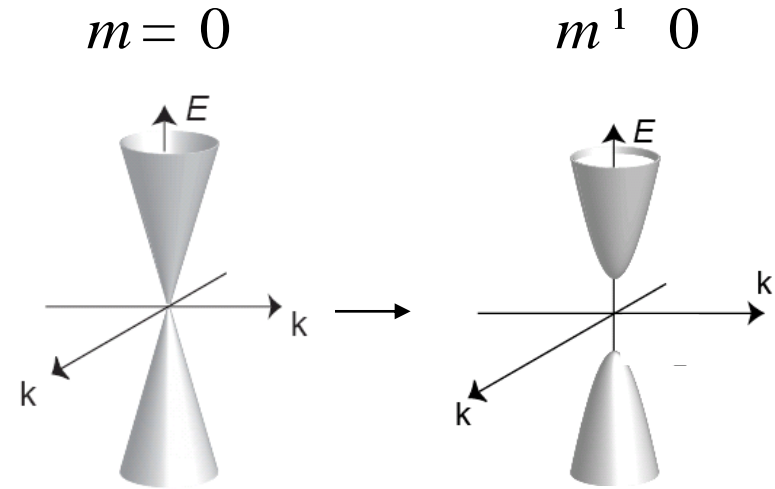
$$H(\mathbf{k}, m) = k_x s_x + k_y s_y + k_z s_z$$

Weyl point moves but gap does not open.

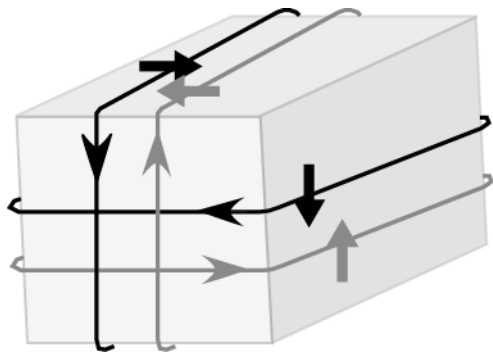
$$(0,0,0) \rightarrow (0,0,-m)$$

← Monopole charge (in 3D k-space) is conserved

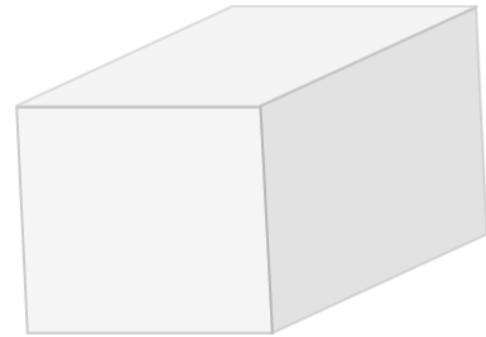
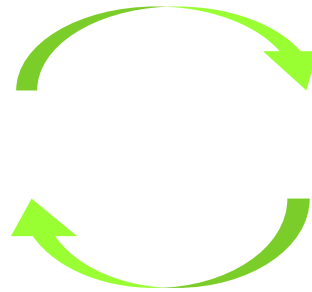
3D Weyl node is topological.



NI-TI phase transitions and Weyl semimetals



TI: topological insulator



NI: normal insulator

SM, New J. Phys. ('07).

SM. Kuga, PRB ('08)

SM, Physica E43, 748 ('11)

Z_2 topological number ν

$\nu=0$: normal insulator (NI)
 $\nu=1$: topological insulator (TI)

(A) systems without inversion symmetry

$$(-1)^\nu = \prod_i \frac{\sqrt{\det[w(\Gamma_i)]}}{\text{Pf}[w(\Gamma_i)]}$$

$$w_{mn}(\vec{k}) = \langle u_{-k,m} | \Theta | u_{k,n} \rangle \quad \Gamma_i : \text{TRIM}$$

Fu, Kane, PRB(2006)

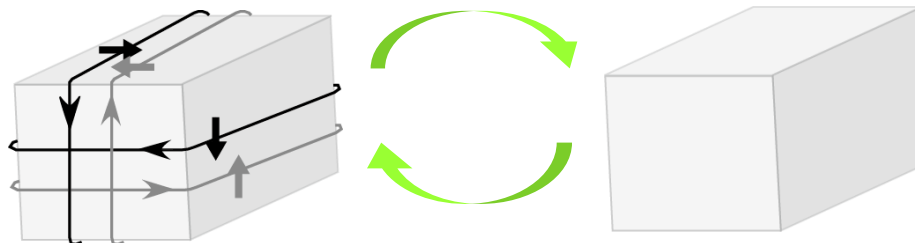
(B) systems with inversion symmetry

$$(-1)^\nu = \prod_i \prod_{m=1}^N \xi_{2m}(\Gamma_i) \quad \text{Parity eigenvalue } +1 \text{ or } -1$$

Fu, Kane, PRB(2007)

different formulae between (A) & (B)

→ TI-NI phase transition in (A) & (B)

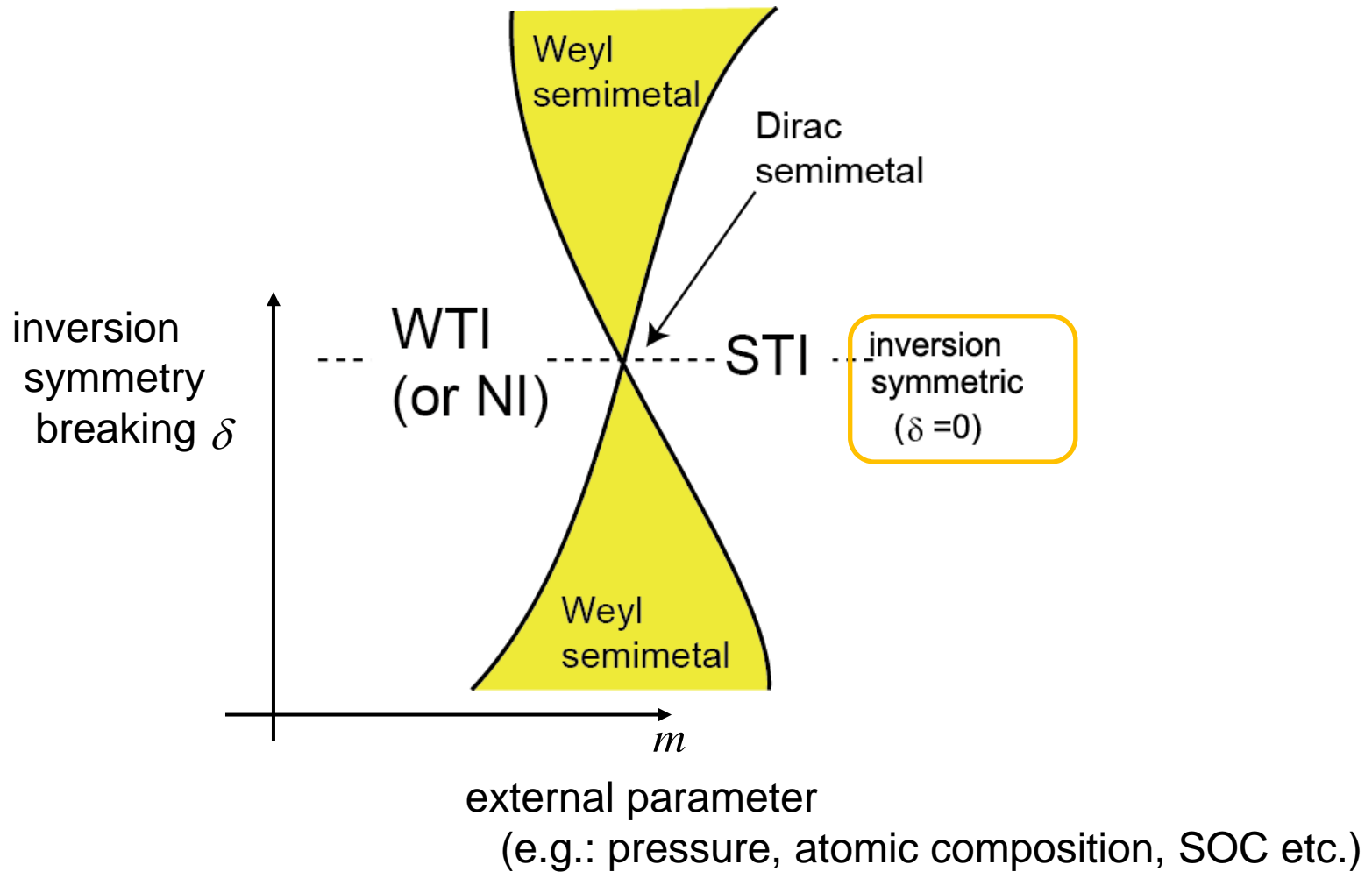


TI: topological insulator

NI: normal insulator

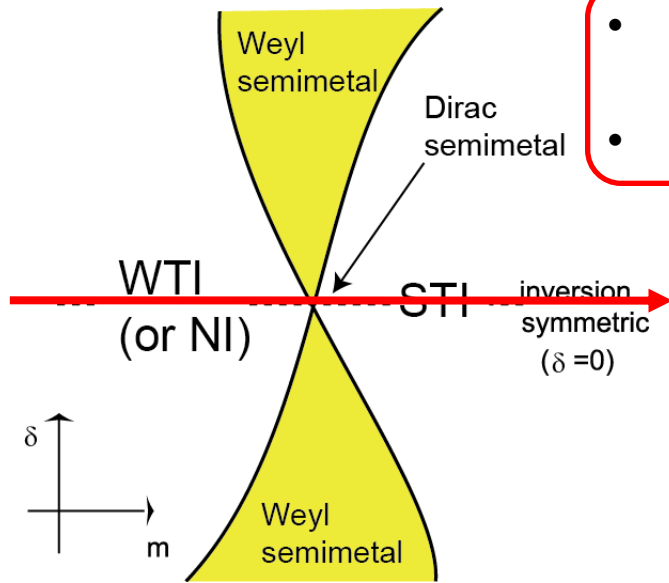
Universal phase diagram in 3D

SM, New J. Phys. ('07).
SM. Kuga, PRB ('08)
SM, Physica E43, 748 ('11)

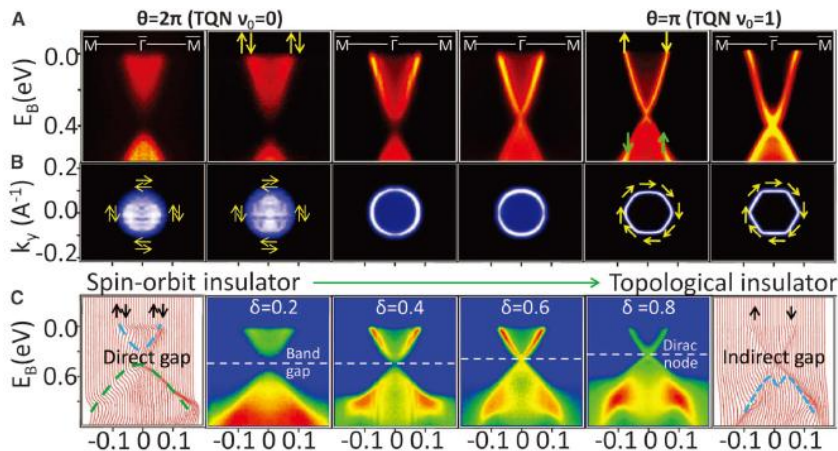
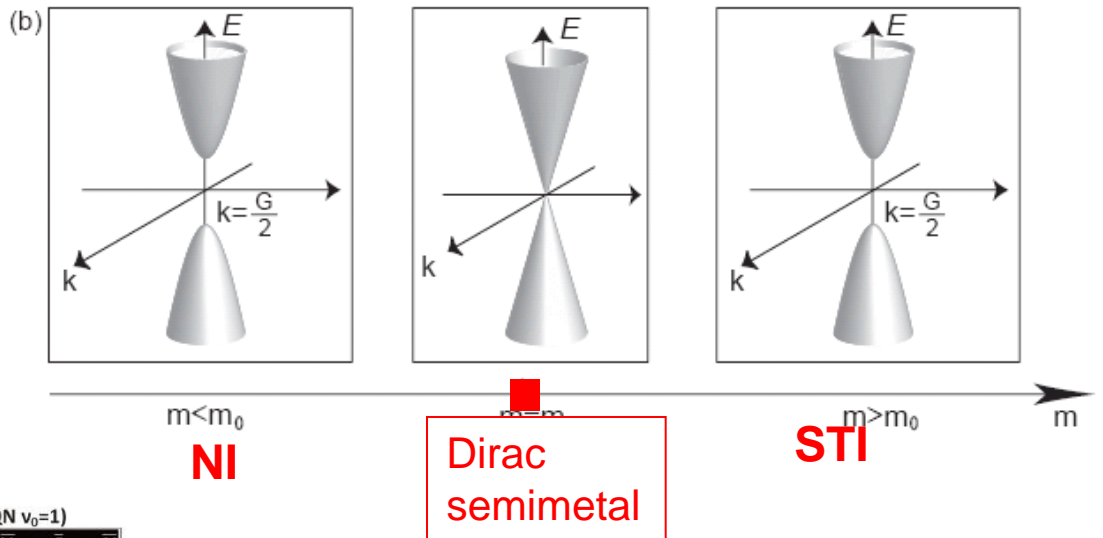


Systems with inversion symmetry

- Gap closes at TRIM
inversion of bands with opposite parities.
- Insulator-to-insulator transition



e.g. $\text{TlBi}(\text{S}_{1-x}\text{Se}_x)_2$

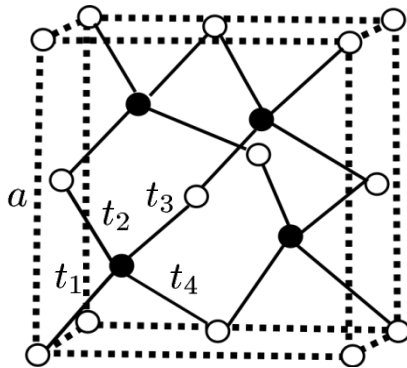


Lattice model: Fu-Kane-Mele model + staggered on-site energy

$$H = \sum_{\langle i,j \rangle} t_{ij} c_i^\dagger c_j + i \frac{8\lambda_{so}}{a^2} \sum_{\langle\langle i,j \rangle\rangle} c_i^\dagger \mathbf{s} \cdot (\mathbf{d}_{ij}^1 \times \mathbf{d}_{ij}^2) c_j + \lambda_v \sum_i \xi_i c_i^\dagger c_i$$

Fu-Kane-Mele model
(PRL98, 106803 (2007))

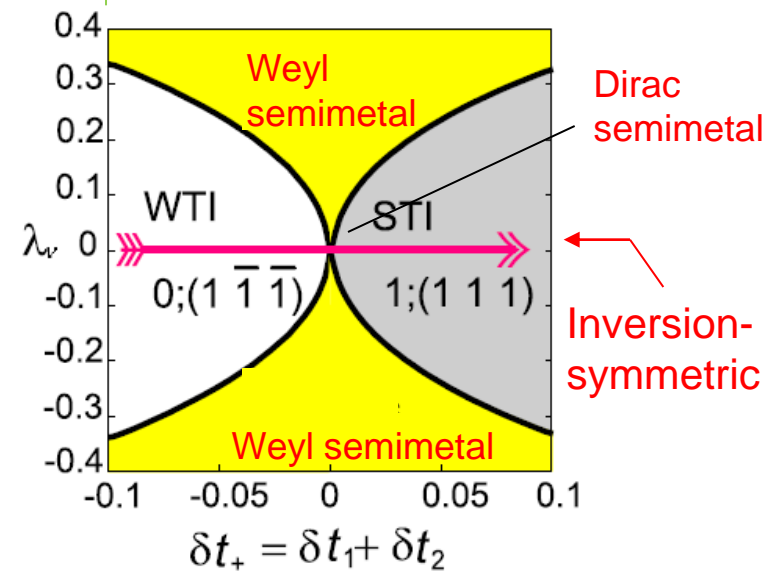
- Diamond lattice
- nearest neighbor: spin-indep. hopping
- next nearest neighbor: spin-orbit coupling



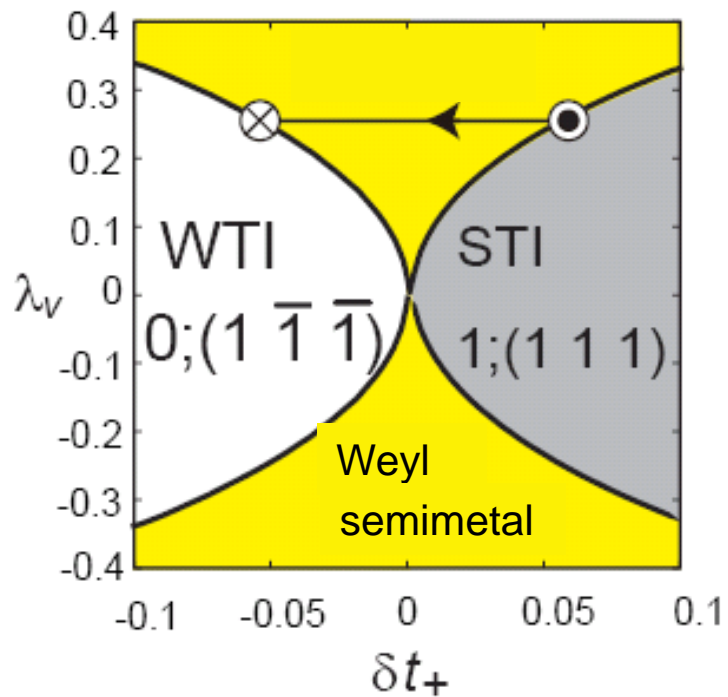
On-site staggered potential
→ breaks inversion



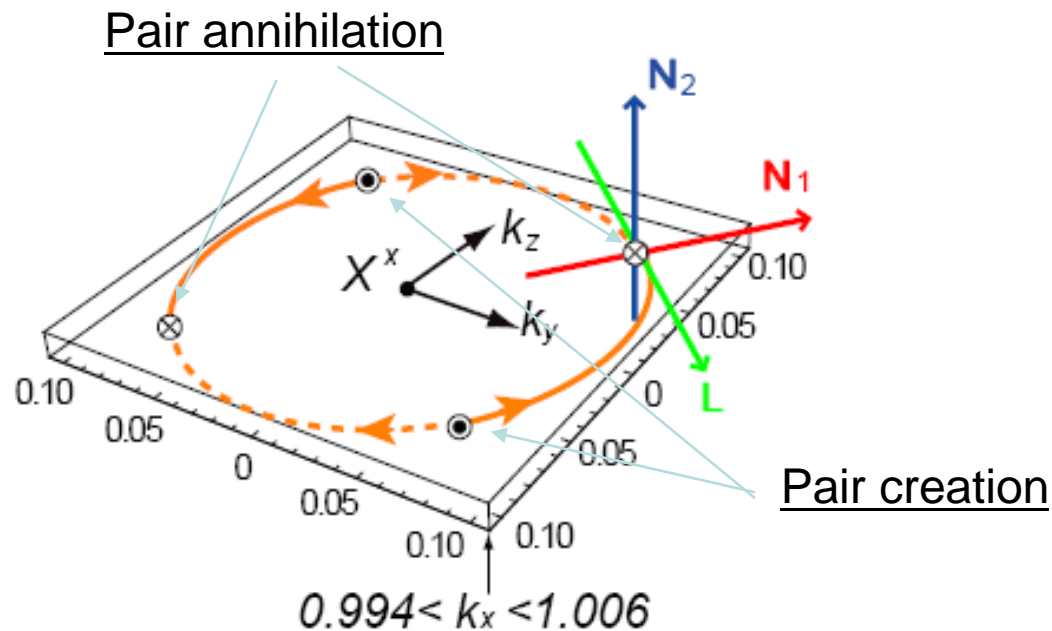
Weyl semimetal appears!
(SM, Kuga,
PRB78, 165313(2008))



Fu-Kane-Mele model
+ inversion-symmetry breaking



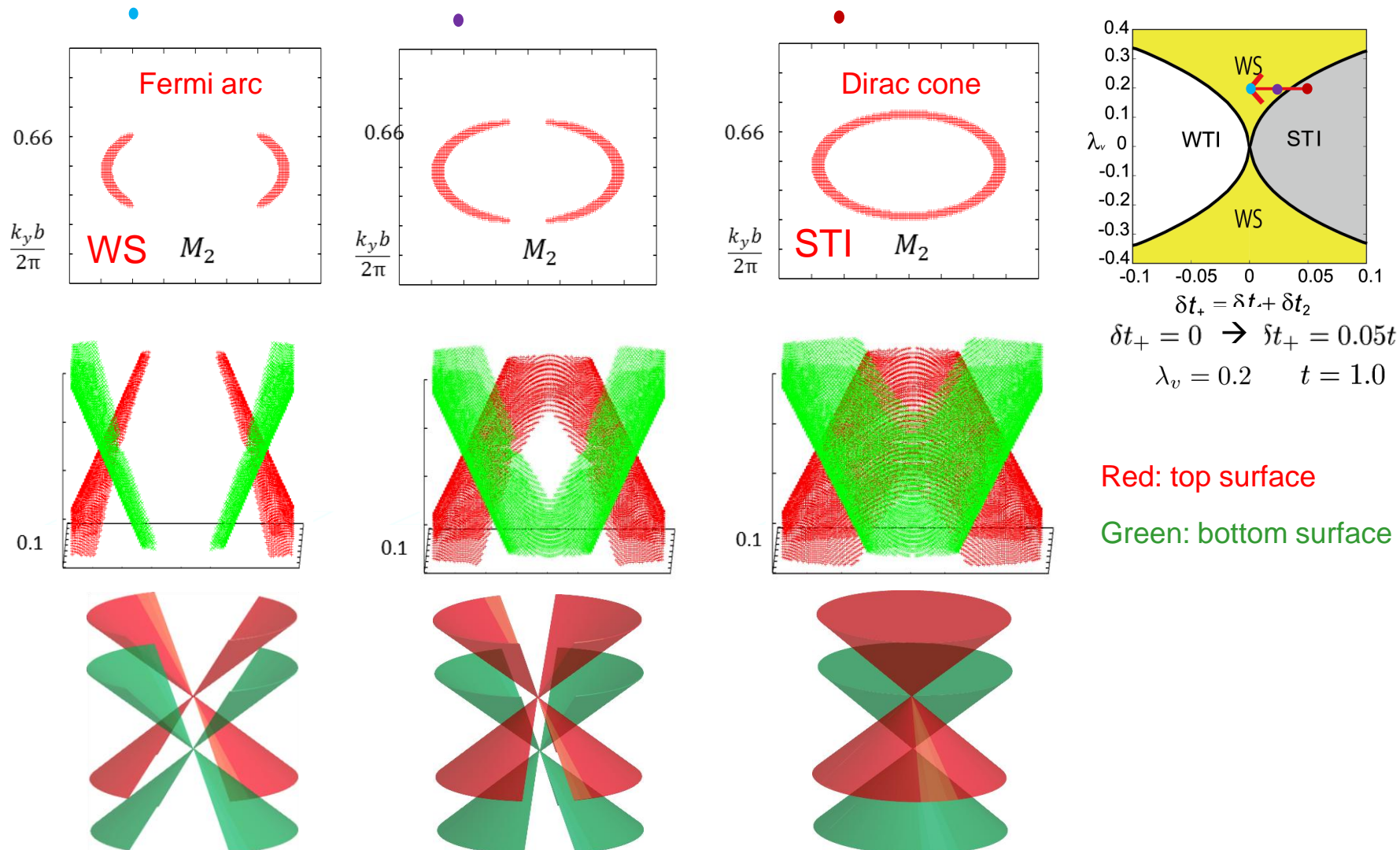
k-space trajectory of the monopoles



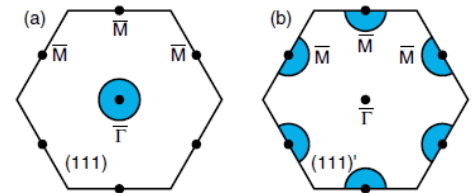
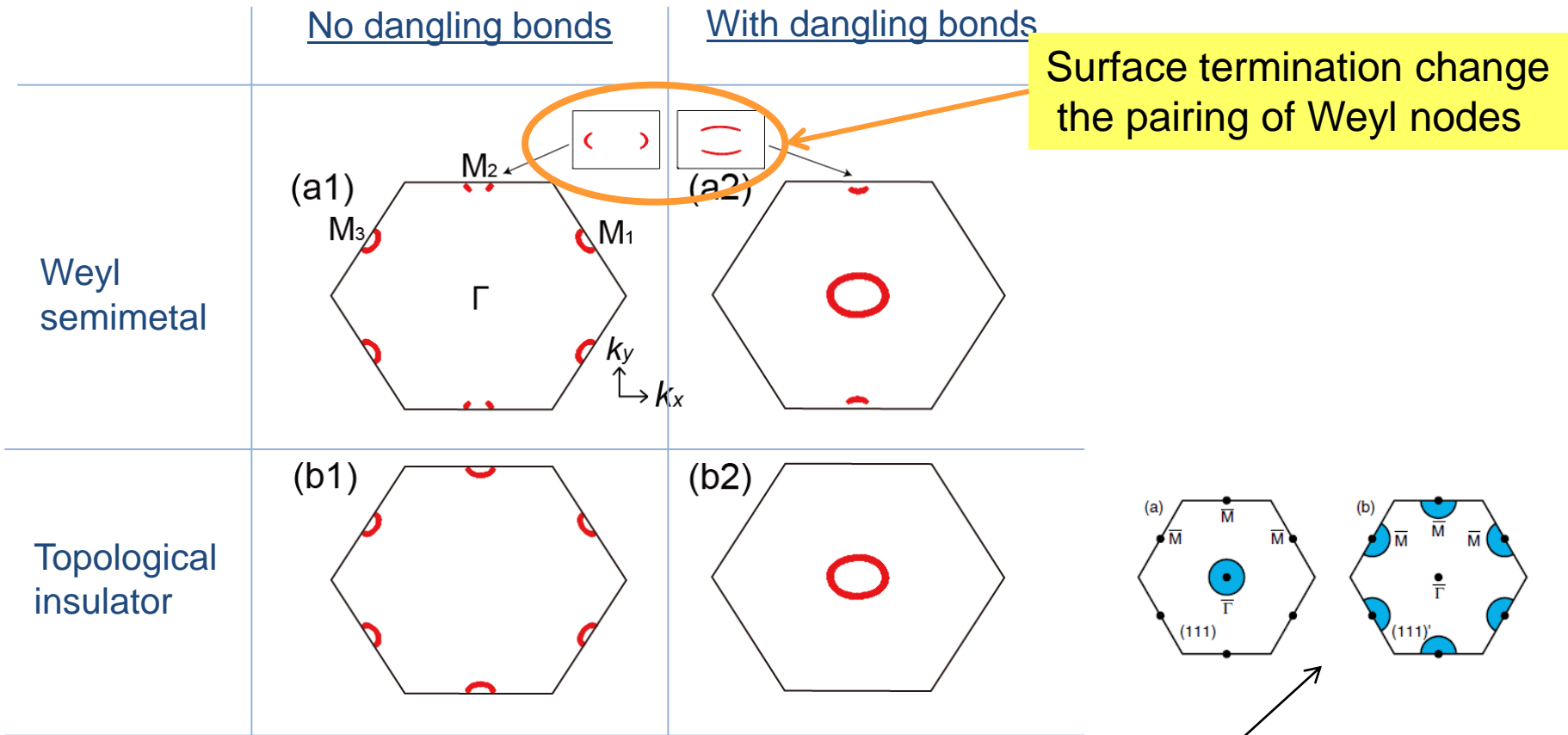
Evolution of surface states

Fermi arcs in the Weyl semimetal \rightarrow (merge) \rightarrow Dirac cones in the TI phase

Okugawa, Murakami, PRB (2014)



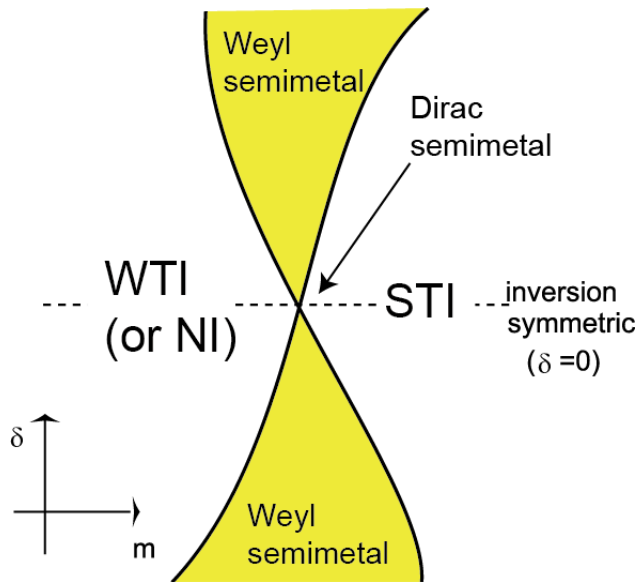
Change of surface terminations



Surface Fermion parity \rightarrow
 surface termination **changes the inside and outside of surface FS.**
 (for inversion symmetric systems)
 Teo, Fu, Kane, PRB78, 045426 (2008)

Universal phase diagram in 3D

SM, New J. Phys. ('07).
SM. Kuga, PRB ('08)
SM, Physica E43, 748 ('11)



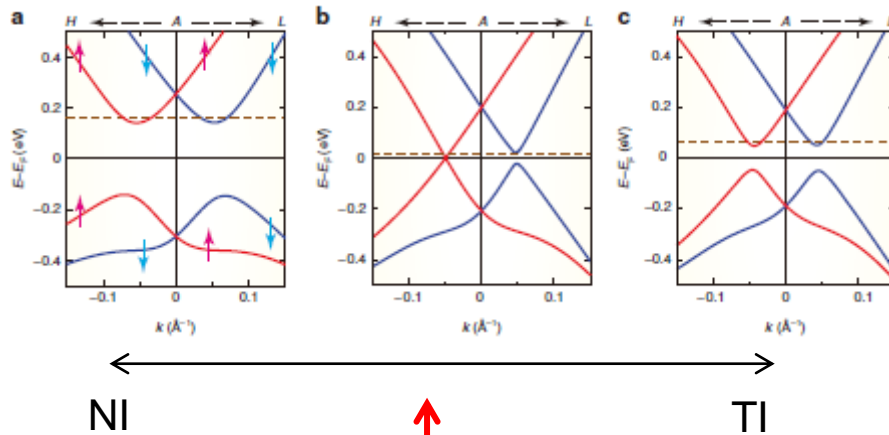
Only the inversion and time-reversal symmetries are considered.

Question:

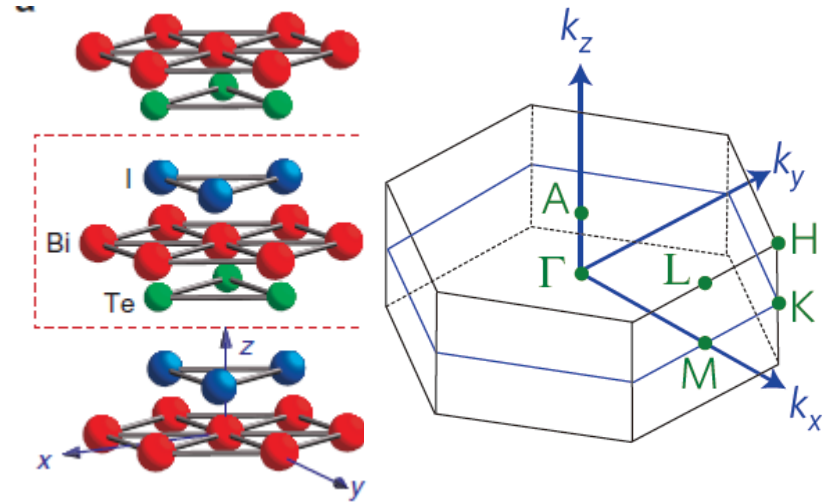
Is it valid for crystals with crystallographic symmetries?

BiTeI at high pressure: ab initio calc.

Bahramy, Nat. Commun. 3, 679 (2012)
 Yang et al. PRL 110, 086402 (2013)

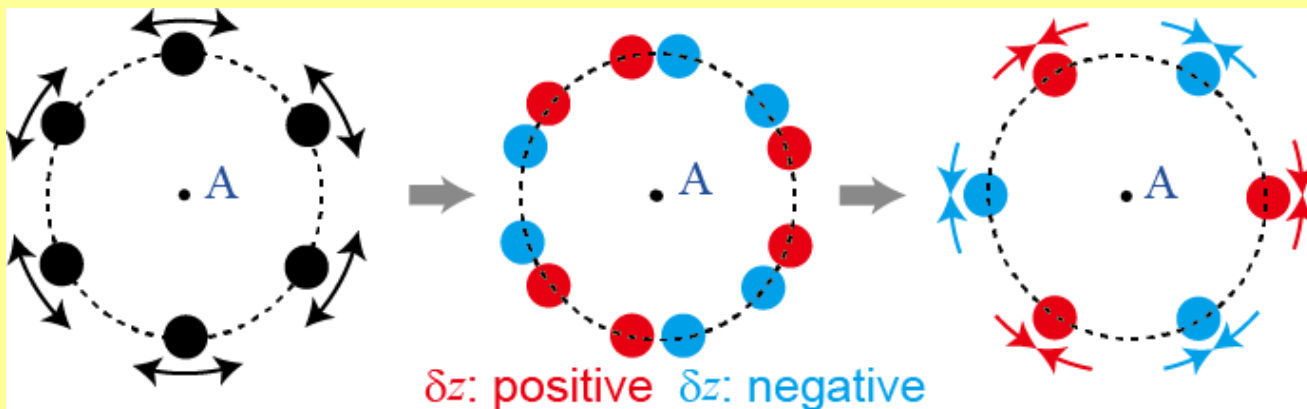


Phase transition at $p=p_c$



No Inversion symmetry

Weyl nodes move with increasing pressure

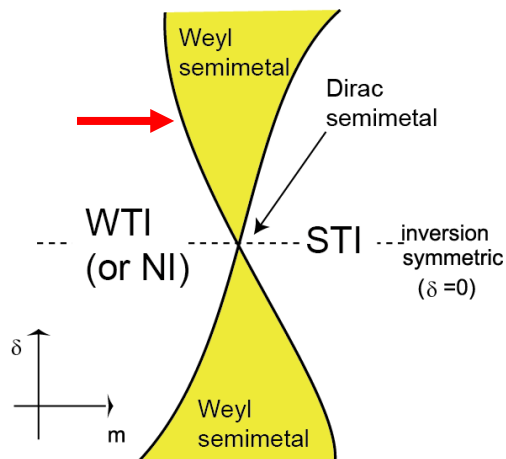
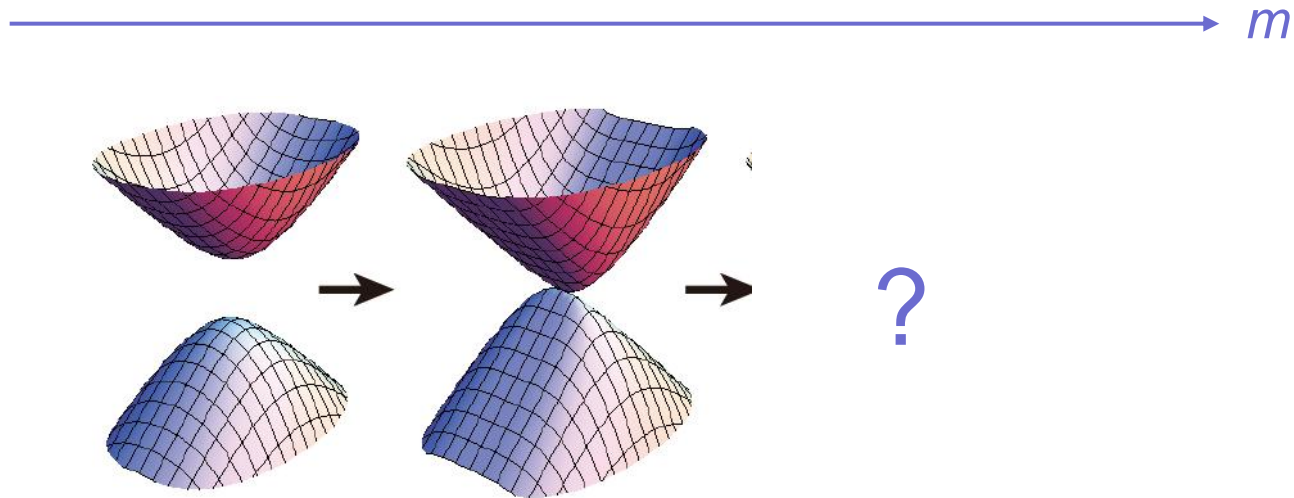


between A and H
 at $p=p_c$
 metal phase

Search for Weyl semimetals without inversion symmetry

Start from any band insulator

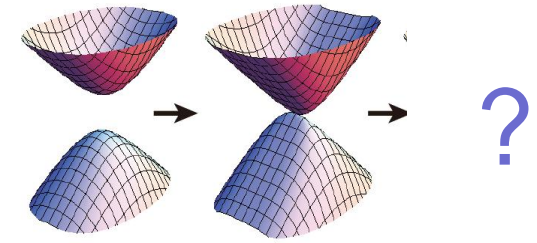
→ suppose a gap closes by changing a parameter m



Classification by space groups & k -points.

230 space groups

138 space groups without inversion sym.



1	2	3	4	5	6	7	8	9	10	11	12	13	14	15	16	17	18	19	20
21	22	23	24	25	26	27	28	29	30	31	32	33	34	35	36	37	38	39	40
41	42	43	44	45	46	47	48	49	50	51	52	53	54	55	56	57	58	59	60
61	62	63	64	65	66	67	68	69	70	71	72	73	74	75	76	77	78	79	80
81	82	83	84	85	86	87	88	89	90	91	92	93	94	95	96	97	98	99	100
101	102	103	104	105	106	107	108	109	110	111	112	113	114	115	116	117	118	119	120
121	122	123	124	125	126	127	128	129	130	131	132	133	134	135	136	137	138	139	140
141	142	143	144	145	146	147	148	149	150	151	152	153	154	155	156	157	158	159	160
161	162	163	164	165	166	167	168	169	170	171	172	173	174	175	176	177	178	179	180
181	182	183	184	185	186	187	188	189	190	191	192	193	194	195	196	197	198	199	200
201	202	203	204	205	206	207	208	209	210	211	212	213	214	215	216	217	218	219	220
221	222	223	224	225	226	227	228	229	230										

No inversion sym.

156 $P3m1$ C_{3i}^1

($F1$; $K6$; $K7$; $M5$; $Z1$.)

- Γ $G_{12}^4: \{C_3^+ | 000\}, \{\sigma_{v1} | 000\}; 3, 3; 4, 3; 6, 2: a.$
- M $G_4^1 \otimes T_2: \{\sigma_{v1} | 000\}; t_2: 2, 3; 4, 3: b.$
- A $G_{12}^4 \otimes T_2: \{C_3^+ | 000\}, \{\sigma_{v1} | 000\}; t_3: 3, 3; 4, 3; 6, 2: a.$
- L $G_4^1 \otimes T_2: \{\sigma_{v1} | 000\}; t_2 \text{ or } t_3: 2, 3; 4, 3: b.$
- K $G_6^1 \otimes T_3: \{C_3^+ | 000\}; t_1 \text{ or } t_2: 2, 2; 4, 2; 6, 2: a.$
- H $G_6^1 \otimes T_3 \otimes T_2: \{C_3^+ | 000\}; t_1 \text{ or } t_2; t_3: 2, 2; 4, 2; 6, 2: a.$
- Δ^x $G_{12}^4: (C_3^+, 0), (\sigma_{v1}, 0); 3, x; 4, x; 6, x: a.$
- U^x $G_4^1: (\sigma_{v1}, 0); 2, x; 4, x: b.$
- P^x $G_6^1: (C_3^+, 0); 2, x; 4, x; 6, x: a.$
- T^x $G_2^1: (\bar{E}, 0); 2, 2: a.$
- S^x $G_2^1: (\bar{E}, 0); 2, 2: a.$
- T'^x $G_2^1: (\bar{E}, 0); 2, 2: a.$
- S'^x $G_2^1: (\bar{E}, 0); 2, 2: a.$
- Σ^x $G_4^1: (\sigma_{v1}, 0); 2, x; 4, x: b.$
- R^x $G_4^1: (\sigma_{v1}, 0); 2, x; 4, x: b.$

} high-symmetry points (TRIM)
 } high-symmetry points (non TRIM)
 } high-symmetry lines

“The Mathematical Theory of Symmetry in Solids”,
 Bradley, Cracknell

Each k point → little group → irreps.

Gap closing in systems without inversion symmetry.

Start from an insulator \rightarrow the gap closes by changing a parameter m

effective model

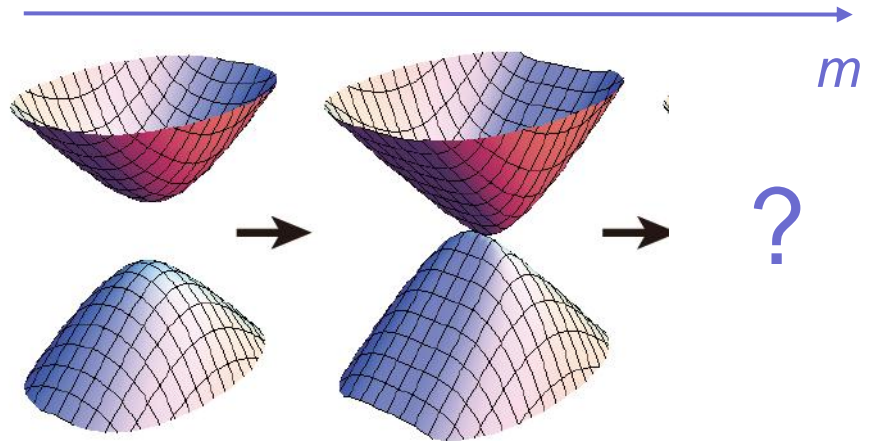
$$H(\vec{k}, m) = \begin{pmatrix} * & * & * & * & * \\ * & * & * & * & * \\ * & * & * & * & * \\ * & * & * & * & * \\ * & * & * & * & * \end{pmatrix}$$

irrep.

R_c

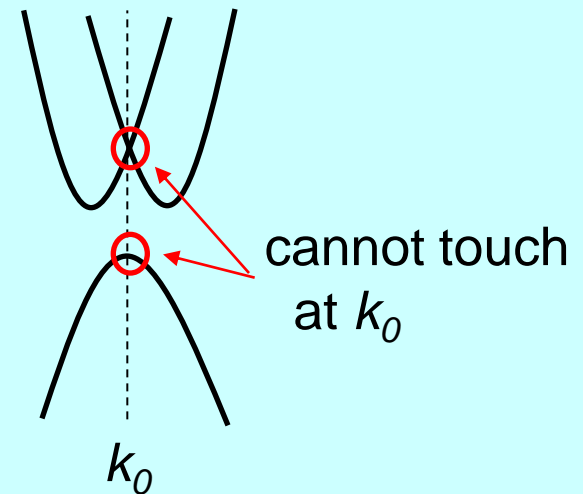
irrep.

R_v

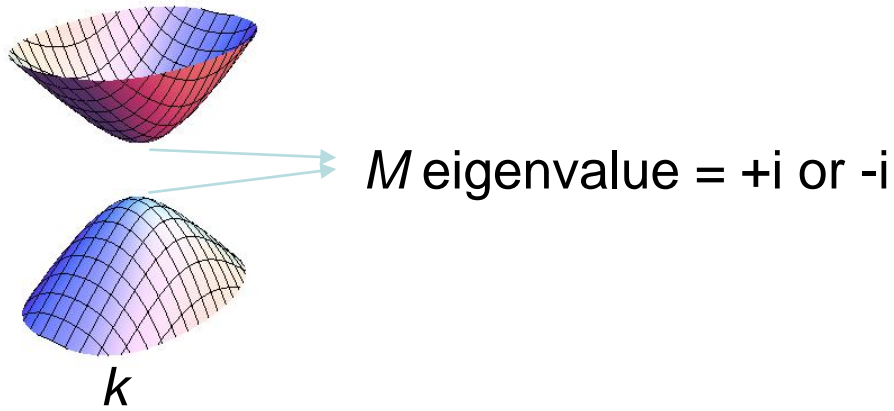


R_c and R_v should be one-dimensional
(Otherwise the gap does not close at k_0)

$$H(\vec{k}, m) = \begin{pmatrix} * & * \\ * & * \end{pmatrix} = \sum_i a_i(\vec{k}, m) \sigma_i$$

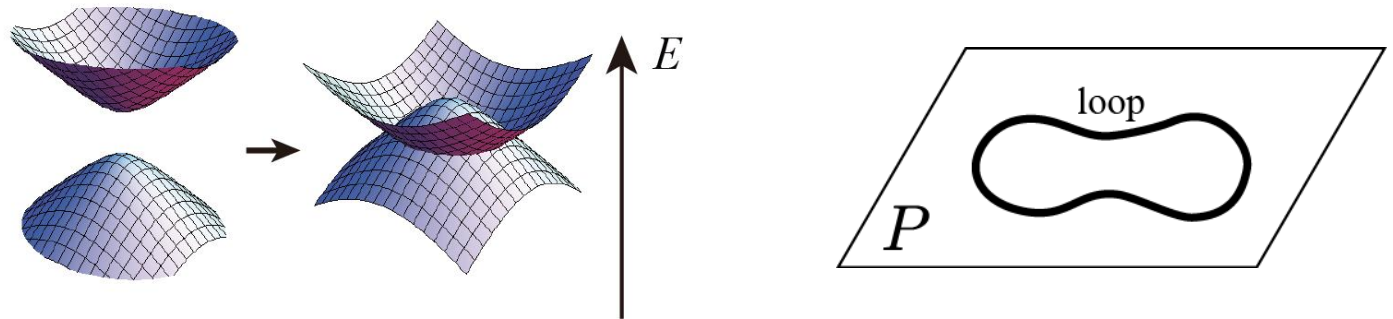


(Example #1): mirror symmetry (i.e. k : invariant under M)

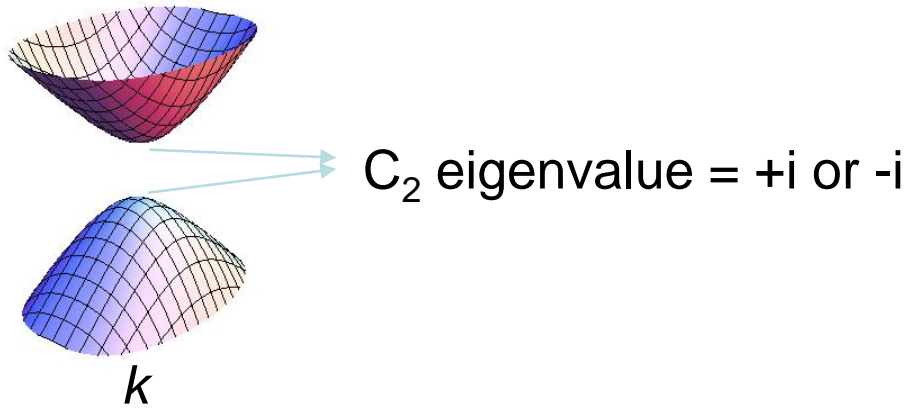


(i) Same signs of M
gap **cannot** close at k – level repulsion

(ii) Different signs of M
nodal-line semimetal
(gap closing along a loop on a mirror plane)

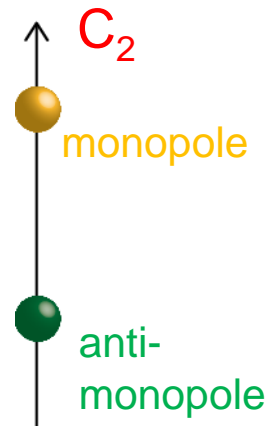
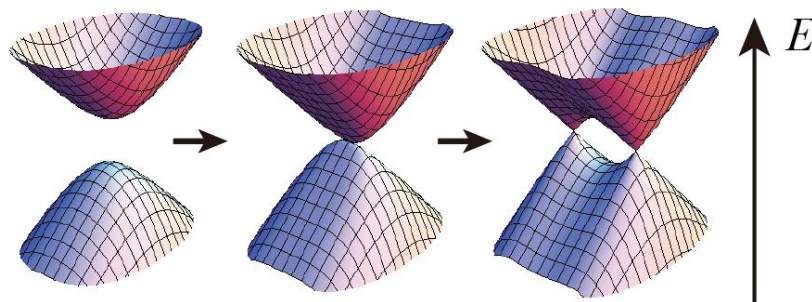


(Example #2): C_2 symmetry (i.e. k : invariant under C_2)

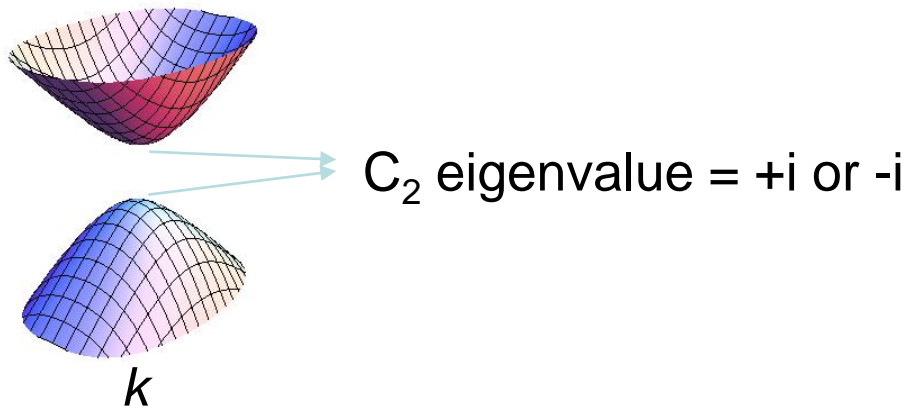


(i) Same signs of C_2
gap **cannot** close at k – level repulsion

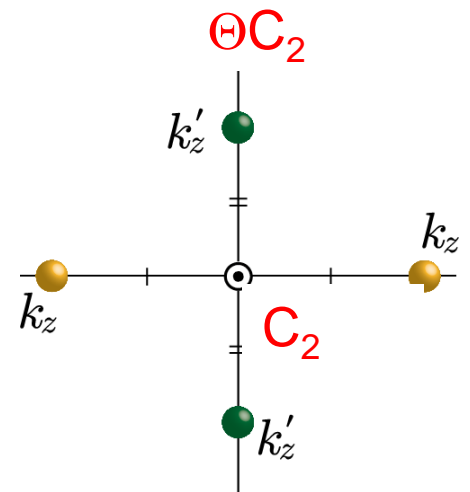
(ii) Different signs of C_2
gap closing
→ Weyl semimetal
pair creation of Weyl nodes
→ move along C_2 line



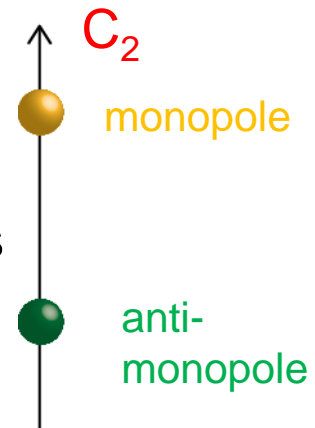
(Example #3): C_2 and ΘC_2 symmetries



- (i) Same signs of C_2
 no level repulsion
 Weyl semimetal
 two pairs of Weyl nodes \rightarrow

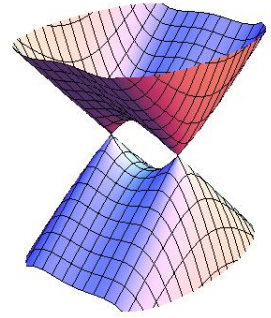


- (ii) Different signs of C_2
 Weyl semimetal
 one pair of Weyl nodes along C_2 axis

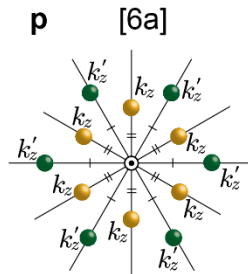
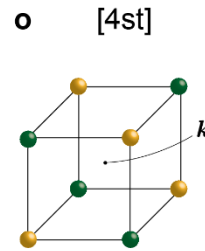
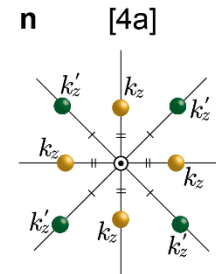
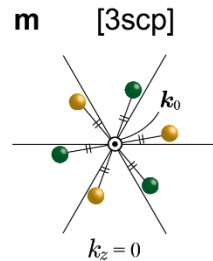
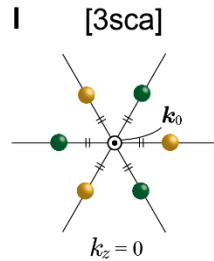
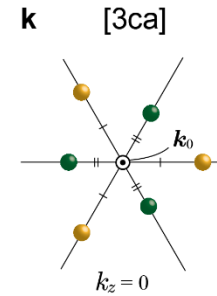
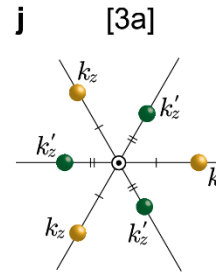
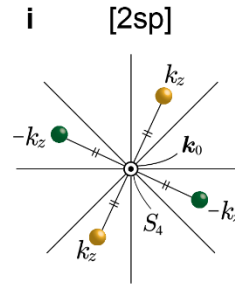
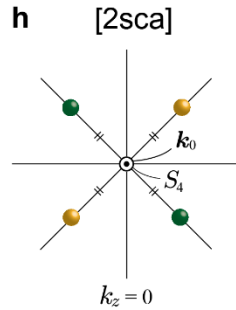
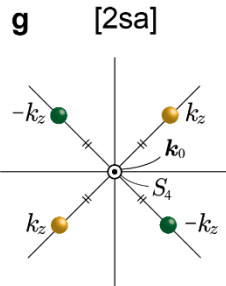
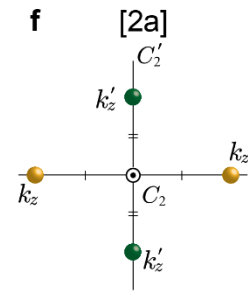
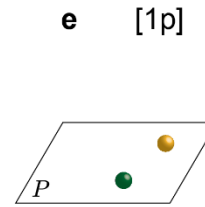
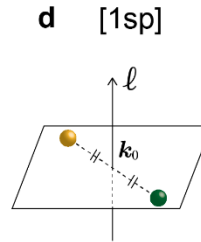
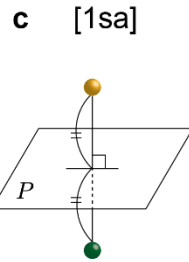
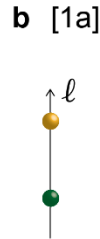
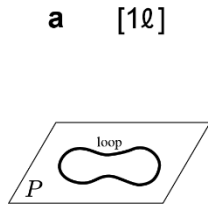
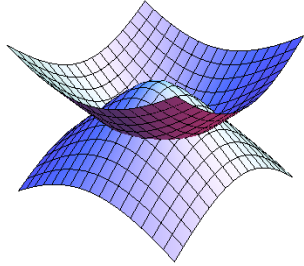


Systems without inversion symmetry

→ Classification of parametric gap-closing



Nodal line semimetal



Weyl semimetal

tetragonal

	point	line
75	$P4$	$\Delta UESYT:1p$ AVW:ij;1a
76	$P4_1$	$\Delta SY:1p$ AVW:ij;1a
77	$P4_2$	$\Delta UESYT:1p$ AVW:ij;1a
78	$P4_3$	$\Delta SY:1p$ AVW:ij;1a
79	$I4$	AVW:ij;1a $\Sigma F\Delta UY:1p$
80	$I4_1$	AVW:ij;1a $\Sigma F\Delta UY:1p$
81	$P\bar{4}$	$\Delta UESYT:1p$ W:ij;1a
82	$\bar{I}4$	W:ij;1a $\Sigma F\Delta UY:1p$
89	$P4_{22}$	$\Delta UESYTW:ii;2a,ij;1a$ AV:ii;4a,ij;1a
90	$P4_{212}$	$\Delta U\Sigma S:ii;2a,ij;1a$ A:ii;4a,ij;1a
91	$P4_122$	$\Delta \Sigma YW:ii;2a,ij;1a$ AV:ii;4a,ij;1a
92	$P4_12_12$	$\Delta \Sigma:ii;2a,ij;1a$ A:ii;4a,ij;1a
93	$P4_222$	$\Delta UESYTW:ii;2a,ij;1a$ AV:ii;4a,ij;1a
94	$P4_22_12$	$\Delta U\Sigma S:ii;2a,ij;1a$ A:ii;4a,ij;1a
95	$P4_322$	$\Delta \Sigma YW:ii;2a,ij;1a$ AV:ii;4a,ij;1a
96	$P4_32_12$	$\Delta \Sigma:ii;2a,ij;1a$ A:ii;4a,ij;1a
97	$I4_{22}$	AV:ii;4a,ij;1a $W\Sigma F\Delta UY:ii;2a,ij;1a$ Q:ij;1a
98	$I4_122$	P:(2,3);4a AV:ii;4a,ij;1a $W\Sigma F\Delta UY:ii;2a,ij;1a$ Q:ij;1a
99	$P4_{mm}$	$\Delta UESYT:ii;1sa,ij;1l$
100	$P4_{bm}$	$\Delta U\Sigma S:ii;1sa,ij;1l$ W:[3]
101	$P4_2cm$	$\Delta \Sigma SY:ii;1sa,ij;1l$
102	$P4_2nm$	$\Delta \Sigma EST:ii;1sa,ij;1l$ W:[3]
103	$P4_{cc}$	$\Delta \Sigma Y:ii;1sa,ij;1l$
104	$P4_{nc}$	$\Delta \Sigma T:ii;1sa,ij;1l$ W:[3]
105	$P4_2mc$	$\Delta UESYT:ii;1sa,ij;1l$
106	$P4_2bc$	$\Delta U\Sigma S:ii;1sa,ij;1l$ W:[3]
107	$I4_{mm}$	$\Sigma F\Delta UY:ii;1sa,ij;1l$ Q:1sp
108	$I4_{cm}$	$\Sigma F\Delta UY:ii;1sa,ij;1l$
109	$I4_1md$	P:(13,14);2l W:[3] $\Sigma F\Delta UY:ii;1sa,ij;1l$ Q:1sp
110	$I4_1cd$	W:[3] $\Sigma F\Delta UY:ii;1sa,ij;1l$
111	$P\bar{4}2m$	$\Delta UYTW:ii;2a,ij;1a$ $\Sigma S:ii;1sa,ij;1l$
112	$P\bar{4}2c$	$\Delta UYTW:ii;2a,ij;1a$ $\Sigma:ii;1sa,ij;1l$
113	$P\bar{4}2_1m$	$\Delta U:ii;2a,ij;1a$ $\Sigma S:ii;1sa,ij;1l$
114	$P\bar{4}2_1c$	$\Delta U:ii;2a,ij;1a$ $\Sigma:ii;1sa,ij;1l$
115	$P\bar{4}m2$	$\Delta UYT:ii;1sa,ij;1l$ $\Sigma S:ii;2a,ij;1a$
116	$P\bar{4}c2$	$\Delta Y:ii;1sa,ij;1l$ $\Sigma S:ii;2a,ij;1a$
117	$P\bar{4}b2$	$\Delta U:ii;1sa,ij;1l$ $\Sigma:ii;2a,ij;1a$ W:[3]
118	$P\bar{4}n2$	$\Delta T:ii;1sa,ij;1l$ $\Sigma S:ii;2a,ij;1a$ W:[3]
119	$\bar{I}4m2$	P:[4] $W\Delta UY:ii;2a,ij;1a$ $\Sigma F:ii;1sa,ij;1l$ Q:1sp
120	$\bar{I}4c2$	$W\Delta UY:ii;2a,ij;1a$ $\Sigma F:ii;1sa,ij;1l$
121	$\bar{I}4_2m$	$\Sigma F:ii;2a,ij;1a$ Q:ij;1a $\Delta UY:ii;1sa,ij;1l$
122	$\bar{I}4_2d$	P:[5] W:[3] $\Sigma F:ii;2a,ij;1a$ $\Delta:ii;1sa,ij;1l$ Q:ij;1a

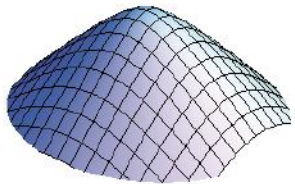
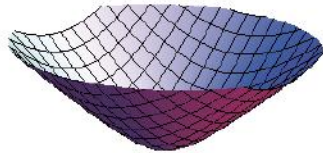
trigonal & hexagonal

	point	line
143	$P3$	$\Delta P:ij;1a$
144	$P3_1$	$\Delta P:ij;1a$
145	$P3_2$	$\Delta P:ij;1a$
146	$R3$	AP:ij;1a
149	$P3_{12}$	$\Delta P:ii;3a,ij;1a$ $UTST'S':1p$ $\Sigma R:ij;1a$
150	$P3_{21}$	KH:(3,4);3ca $\Delta:ii;3a,ij;1a$ $U\Sigma R:1p$ $PTST'S':ij;1a$
151	$P3_112$	$\Delta P:ii;3a,ij;1a$ $UTST'S':1p$ $\Sigma R:ij;1a$
152	$P3_121$	KH:(3,4);3ca $\Delta:ii;3a,ij;1a$ $U\Sigma R:1p$ $PTST'S':ij;1a$
153	$P3_212$	$\Delta P:ii;3a,ij;1a$ $UTST'S':1p$ $\Sigma R:ij;1a$
154	$P3_221$	KH:(3,4);3ca $\Delta:ii;3a,ij;1a$ $U\Sigma R:1p$ $PTST'S':ij;1a$
155	$R32$	AP:ij;3a,ij;1a $\Sigma EQY:ij;1a$
156	$P3m1$	KH:ij;1a $\Delta:(3,4);3l$ $U\Sigma R:ij;1l$ $P:ij;1a$ $TST'S':1sp$
157	$P31m$	$\Delta P:(3,4);3l$ $UTST'S':ij;1l$ $\Sigma R:1sp$
158	$P3c1$	K:ij;1a $\Delta:(3,4);3l$ $P:ij;1a$ $U\Sigma R:ij;1l$ $TT':1sp$
159	$P31c$	$\Delta P:(3,4);3l$ $UTST'S':ij;1l$ $\Sigma:1sp$
160	$R3m$	AP:(3,4);3l $\Sigma EQY:1sp$
161	$R3c$	AP:(3,4);3l $\Sigma Q:1sp$
168	$P6$	$\Delta UP:ij;1a$ $TST'S'\Sigma R:1p$
169	$P6_1$	$\Delta UP:ij;1a$ $TT'\Sigma:1p$
170	$P6_6$	$\Delta UP:ij;1a$ $TT'\Sigma:1p$
171	$P6_2$	$\Delta UP:ij;1a$ $TST'S'\Sigma R:1p$
172	$P6_4$	$\Delta UP:ij;1a$ $TST'S'\Sigma R:1p$
173	$P6_3$	$\Delta UP:ij;1a$ $TT'\Sigma:1p$
174	$P\bar{6}$	KH:[6] $\Delta:(4,4);3scp$ $U:1sp$ $P:ij;1a$ $TST'S'\Sigma R:ij;1l$
177	$P6_{22}$	KH:(3,4);3ca $\Delta:ii;6a,ij;1a$ $UTST'S'\Sigma R:ii;2a,ij;1a$ $P:ii;3a,ij;1a$
178	$P6_122$	K:(3,4);3ca $\Delta:ii;6a,ij;1a$ $UTT'\Sigma:ii;2a,ij;1a$ $P:ii;3a,ij;1a$
179	$P6_622$	K:(3,4);3ca $\Delta:ii;6a,ij;1a$ $UTT'\Sigma:ii;2a,ij;1a$ $P:ii;3a,ij;1a$
180	$P6_222$	KH:(3,4);3ca $\Delta:ii;6a,ij;1a$ $UTST'S'\Sigma R:ii;2a,ij;1a$ $P:ii;3a,ij;1a$
181	$P6_422$	KH:(3,4);3ca $\Delta:ii;6a,ij;1a$ $UTST'S'\Sigma R:ii;2a,ij;1a$ $P:ii;3a,ij;1a$
182	$P6_322$	K:(3,4);3ca $\Delta:ii;6a,ij;1a$ $UTT'\Sigma:ii;2a,ij;1a$ $P:ii;3a,ij;1a$
183	$P6_{mm}$	KH:(3,4);3l P:(3,4);3l $TST'S'\Sigma R:ii;1sa,ij;1l$
184	$P6_{cc}$	K:(3,4);3l P:(3,4);3l $TT'\Sigma:ii;1sa,ij;1l$
185	$P6_3cm$	K:(3,4);3l P:(3,4);3l $TT'\Sigma:ii;1sa,ij;1l$
186	$P6_3mc$	K:(3,4);3l P:(3,4);3l $TT'\Sigma:ii;1sa,ij;1l$
187	$P\bar{6}m2$	KH:[6] $\Delta:(3,4);3l$ (3,3)(4,4);3sca $UTST'S':ii;1sa,ij;1l$ $P:ii;3a,ij;1a$
188	$P\bar{6}c2$	K:[6] $\Delta:(3,4);3l$ (3,3)(4,4);3sca $UTT'\Sigma:ii;1sa,ij;1l$ $P:ii;3a,ij;1a$ $R:[1]$
189	$P\bar{6}2m$	$\Delta:(3,4);3l$ (3,3)(4,4);3sca $U\Sigma R:ii;1sa,ij;1l$ $P:(3,4);3l$
190	$P\bar{6}2c$	H:[8] $\Delta:(3,4);3l$ (3,3)(4,4);3sca $U\Sigma:ii;1sa,ij;1l$ $P:(3,4);3l$ $SS':[1]$

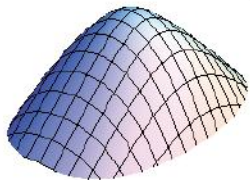
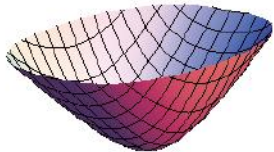
Systems without inversion symmetry

→ Classification of parametric gap-closing

(a) Nodal-line semimetal (← mirror plane)



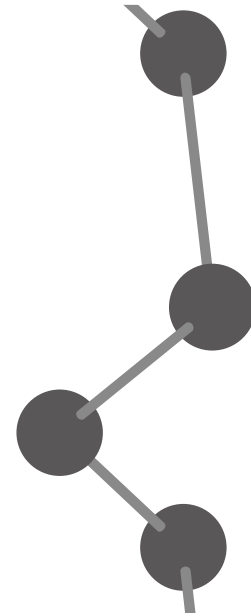
(b) Weyl semimetal



Only two possibilities. No insulator-to-insulator transition happens.

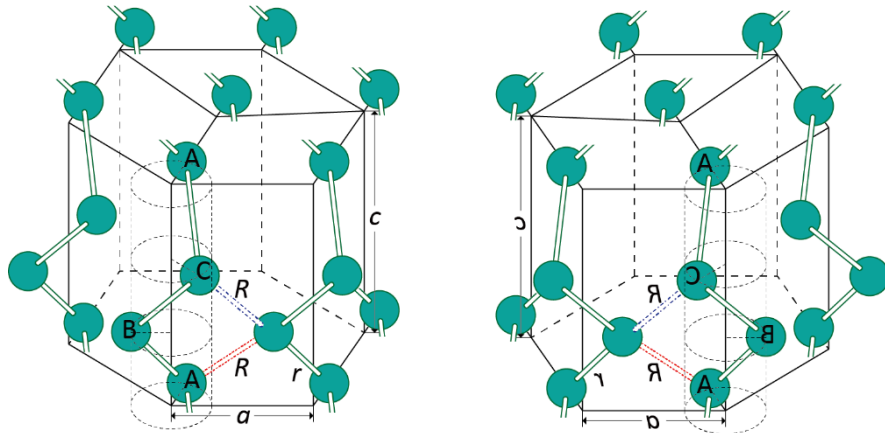
Topological Effects in Tellurium and Selenium

Hirayama, Okugawa, Ishibashi, Murakami, Miyake,
PRL 114, 206401 (2015)



Te : lattice with helical chains

M. Hirayama, R. Okugawa, S. Ishibashi,
S. Murakami, T. Miyake,
PRL (2015)

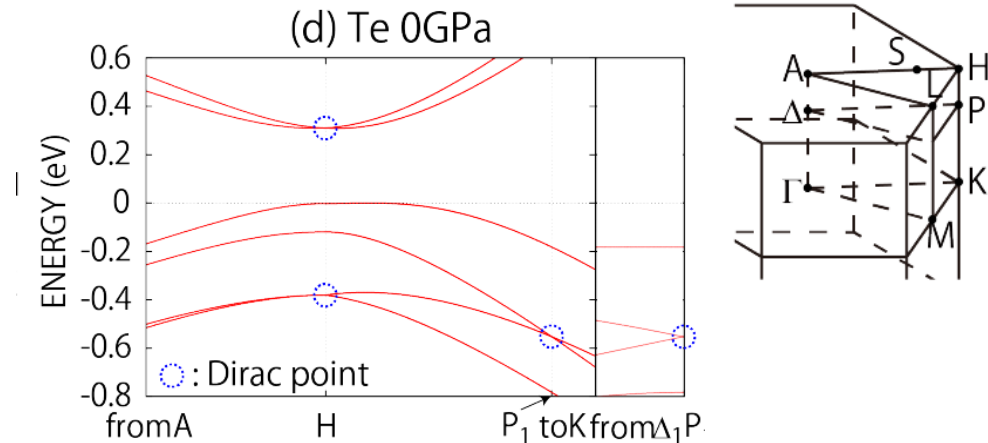
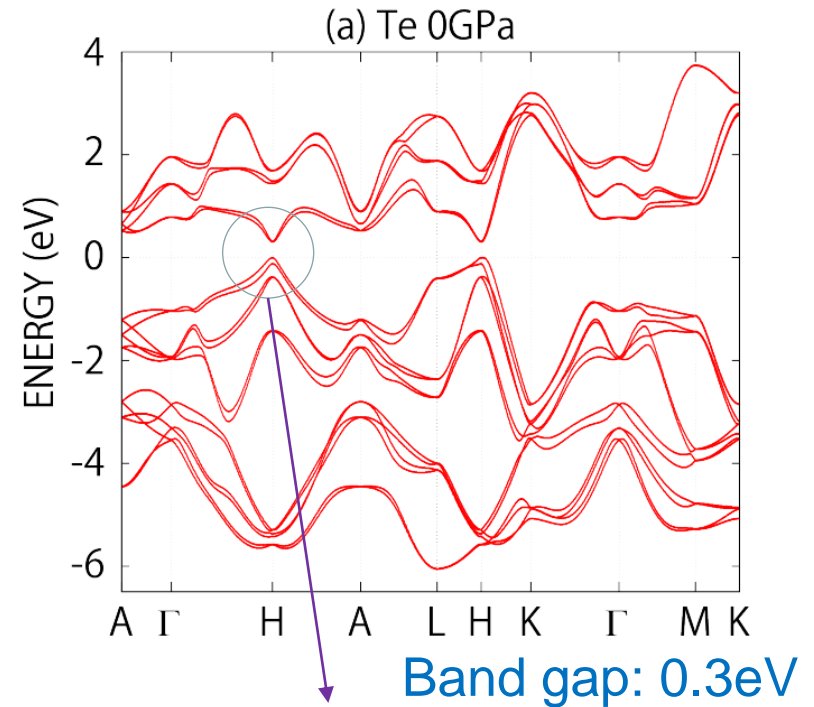


$P3_121$

$P3_221$

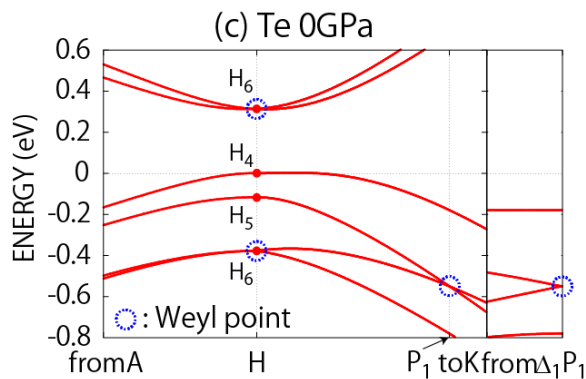
- Lattice with helical chains
- No inversion symmetry
- No mirror symmetry

→ Allow Weyl nodes

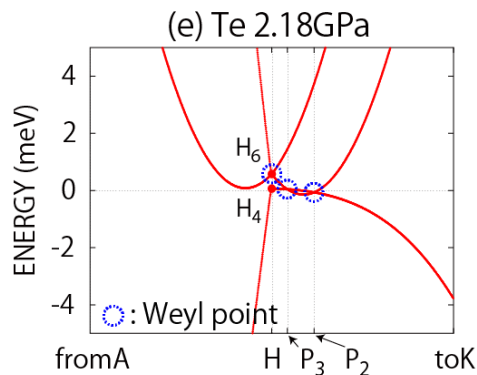


Te becomes Weyl semimetal at high pressure

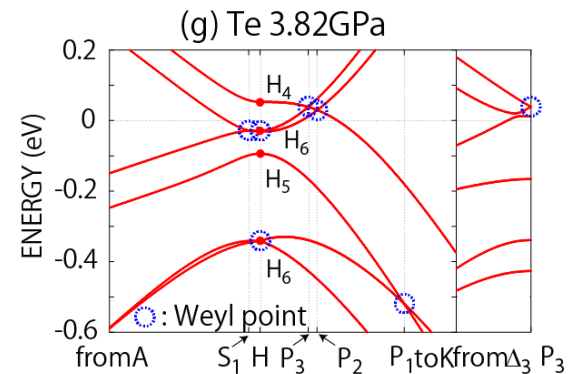
pressure



insulator

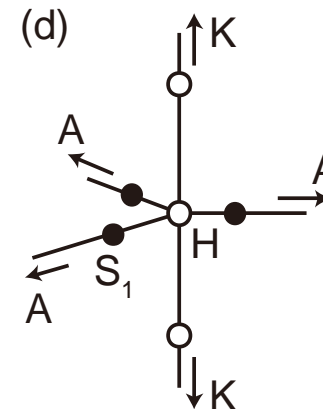
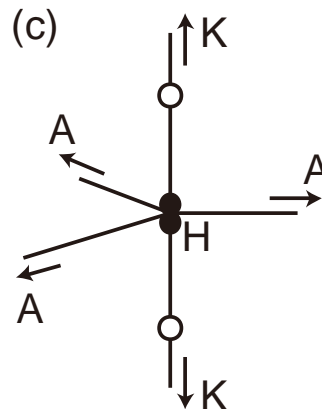
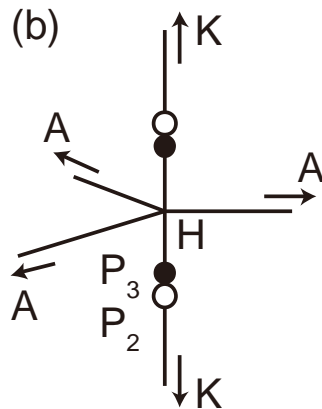
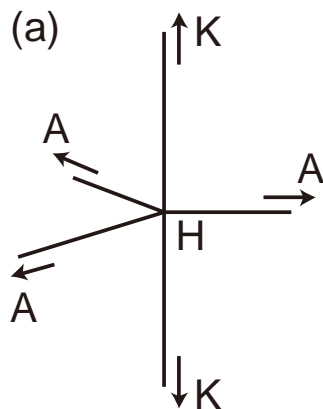


Weyl semimetal

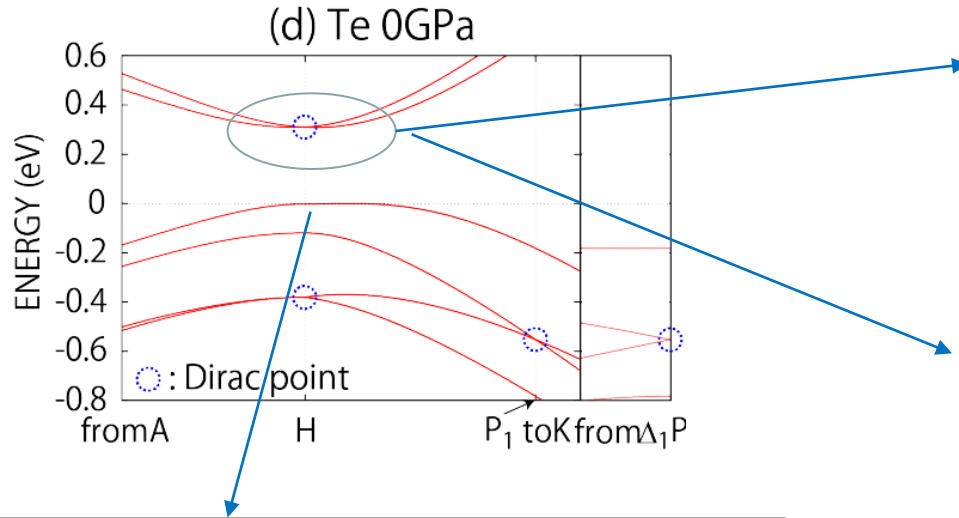


metal

Motion of Weyl Nodes

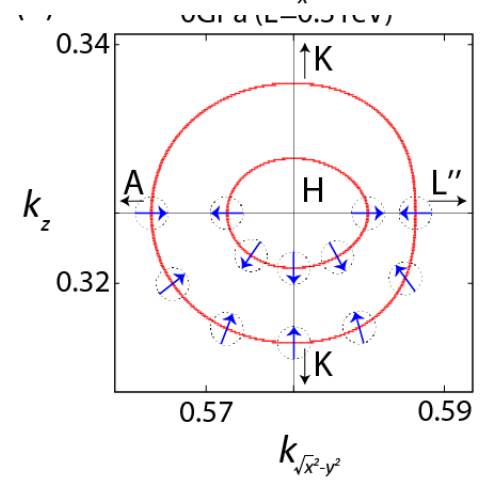
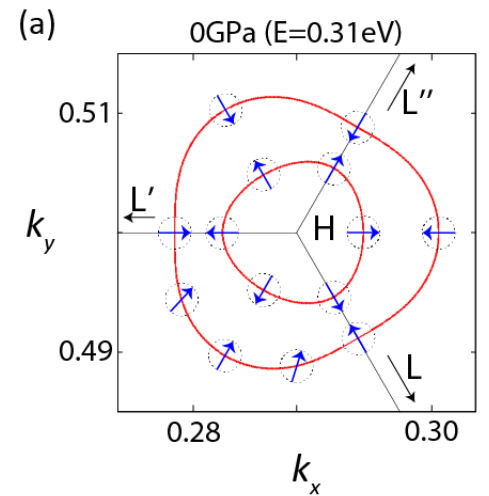
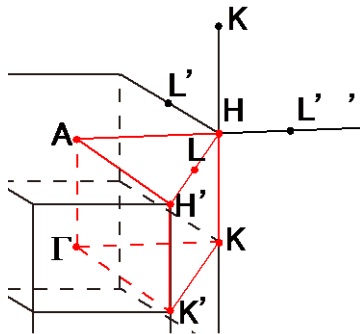


Te: spin structure at ambient pressure



Valence band
spin // z axis

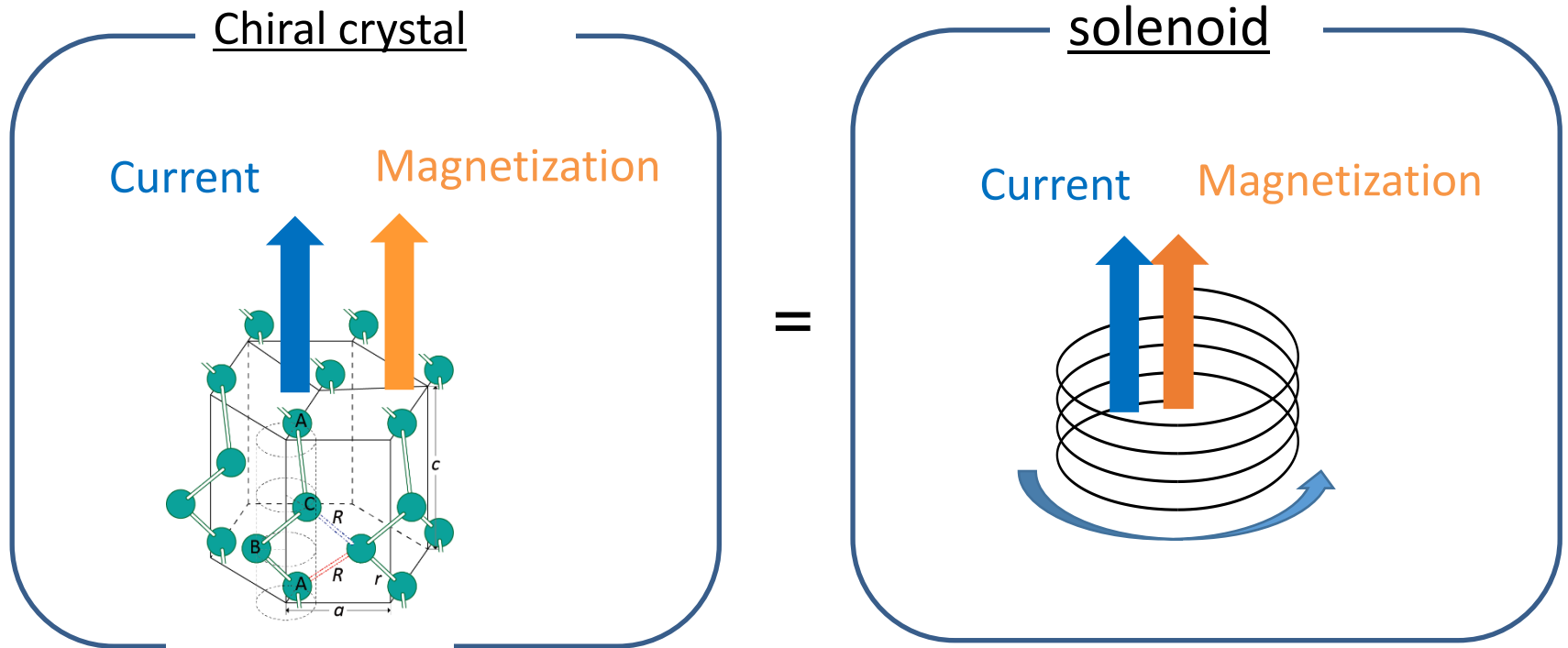
: opposite spins for H and H' points
valley degree of freedom
similar to MoS_2



Conduction band
hedgehog spin structure
: unique to systems without
mirror symmetry

Chiral transport in crystals with helical structure

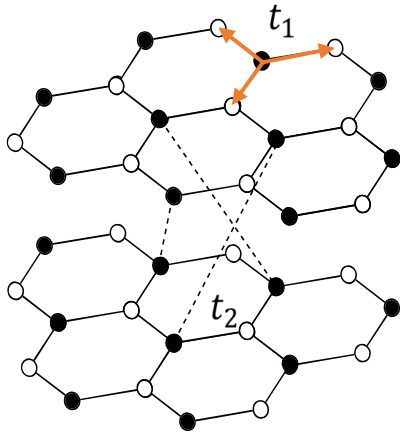
Yoda, Yokoyama, Murakami, *Sci. Rep.* 5, 12024 (2015)



Current-induced orbital magnetization

Model

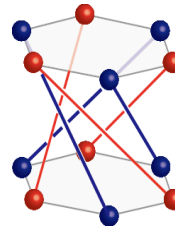
An infinite stack of honeycomb lattice layers with a helical structure



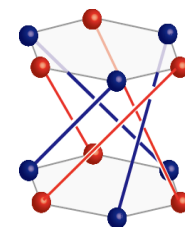
$$H = t_1 \sum_{\langle ij \rangle} c_i^\dagger c_j + t_2 \sum_i \xi_i c_i^\dagger c_j$$

t_1 : nearest neighbor hopping

t_2 : **helical** hopping within
the same sublattice in the neighboring layers



Left-handed



Right-handed

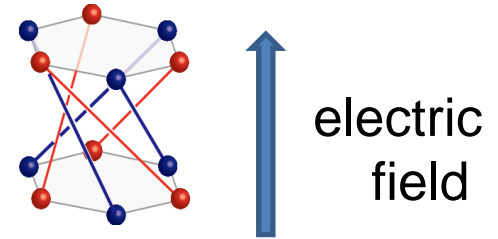
It reduces to Haldane model by replacement: $kz \rightarrow \phi$

Formalism for current induced orbital magnetization

Orbital magnetization (Ceresoli et al, Xiao et al. (2006))

$$\mathbf{M}_{\text{orb}} = \frac{e}{2\hbar} \text{Im} \sum_n \int_{\text{BZ}} \frac{d^3 \mathbf{k}}{(2\pi)^3} f_{n\mathbf{k}} \langle \partial_{\mathbf{k}} u_{n\mathbf{k}} | \times (H_{\mathbf{k}} + \varepsilon_{n\mathbf{k}} - 2\varepsilon_F) | \partial_{\mathbf{k}} u_{n\mathbf{k}} \rangle$$

Apply electric field (// helical axis)



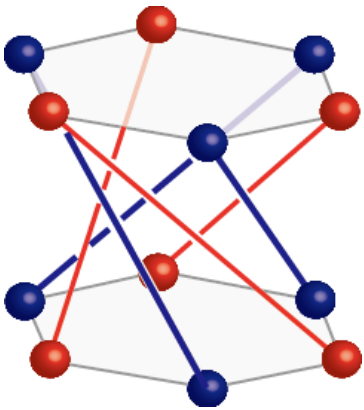
Boltzmann approximation

$$\text{distribution function : } f_{n\mathbf{k}} = f_{n\mathbf{k}}^0 + eE_z \tau v_{n,z} \left. \frac{df}{d\varepsilon} \right|_{\varepsilon=\varepsilon_{n\mathbf{k}}}$$

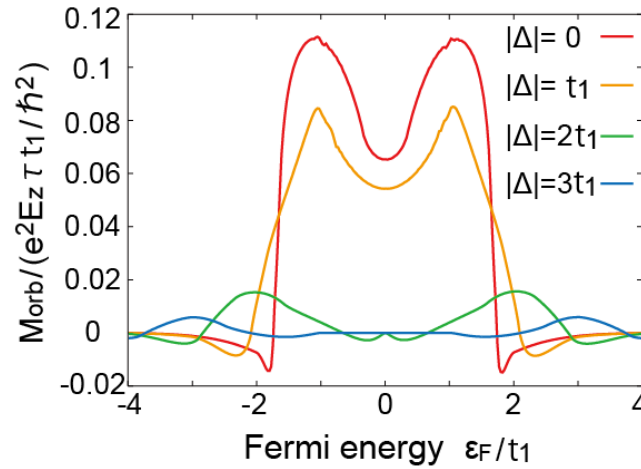
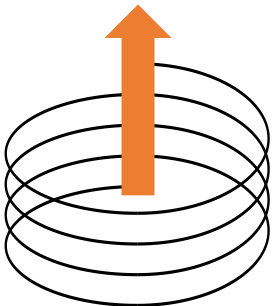
For a metal, the orbital magnetization is induced by an electric current.

▪ Current-induced **orbital** magnetization (no SOC needed)

Left-handed crystal



Current
& magnetization



opposite for the right-handed
and left-handed helix.

Current-induced orbital magnetization

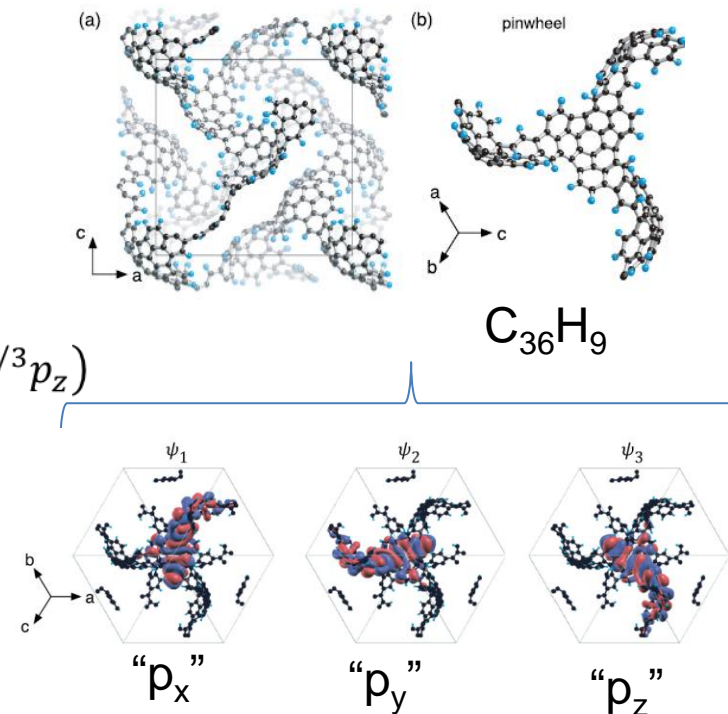
- Inter-site (inter-unit-cell)
 - **Tellurium**: Present work (Yoda, Yokoyama, Murakami, Sci. Rep. (2015))
- Intra-site (intra-unit-cell)
 - **Tellurium** (Shalygin et al., Phys. Solid State 56, 2362 (2012))
 - Current \rightarrow different population for $j_z > 0$ and $j_z < 0$ states
 - **zeolite-templated carbon**
 - Koretsune, Arita, Aoki, PRB **86**, 125207 (2012)

Network of $C_{36}H_9$

At each $C_{36}H_9$

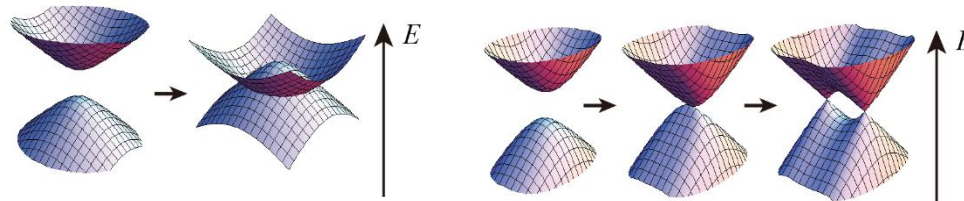
$$\psi_E^\pm = \frac{1}{\sqrt{3}} (p_x + e^{\pm 2\pi i/3} p_y + e^{\pm 4\pi i/3} p_z)$$

$\rightarrow l_z = \pm 1$



Conclusions

- Weyl semimetals (in inversion asymmetric systems)
 - In TI-NI phase transition, Weyl semimetals naturally appear.
 - Under space group symmetry
e.g. Tellurium: Weyl semimetal at high pressure



Murakami, *New J. Phys.* 9, 356 (2007)

Murakami, Kuga, *PRB* 78, 165313 (2008)

Okugawa, Murakami, *Phys. Rev. B* 89, 235315 (2014)

Hirayama et al., *PRL* 114, 206401 (2015)

- Chiral transport in crystals with helical lattice structure
 - analogy with solenoid
 - Current induced orbital & spin magnetization
 - Example:
 - 3D chiral crystals: Tellurium etc.

Yoda, Yokoyama, Murakami, *Sci. Rep.* 5, 12024 (2015)

